

Total scattering cross sections and interatomic potentials for neutral hydrogen and helium on some noble gases

David N. Ruzic and Samuel A. Cohen

Citation: *J. Chem. Phys.* **83**, 5527 (1985); doi: 10.1063/1.449674

View online: <http://dx.doi.org/10.1063/1.449674>

View Table of Contents: <http://jcp.aip.org/resource/1/JCPSA6/v83/i11>

Published by the [American Institute of Physics](#).

Additional information on *J. Chem. Phys.*

Journal Homepage: <http://jcp.aip.org/>

Journal Information: http://jcp.aip.org/about/about_the_journal

Top downloads: http://jcp.aip.org/features/most_downloaded

Information for Authors: <http://jcp.aip.org/authors>

ADVERTISEMENT



Goodfellow
metals • ceramics • polymers • composites
70,000 products
450 different materials
small quantities fast

www.goodfellowusa.com

Total scattering cross sections and interatomic potentials for neutral hydrogen and helium on some noble gases

David N. Ruzic^{a)} and Samuel A. Cohen

Plasma Physics Laboratory, Princeton University, Princeton, New Jersey 08544

(Received 17 June 1985; accepted 22 July 1985)

Measurements of energy-dependent scattering cross sections for 30 to 1800 eV D incident on He, Ne, Ar, and Kr, and for 40 to 850 eV He incident on He, Ar, and Kr are presented. They are determined by using the charge-exchange efflux from the Princeton large torus tokamak as a source of D or He. These neutrals are passed through a gas-filled scattering cell and detected by a time-of-flight spectrometer. The cross section for scattering greater than the effective angle of the apparatus (≈ 20 mrad) is found by measuring the energy-dependent attenuation of D or He as a function of pressure in the scattering cell. The interatomic potential is extracted from the data.

Neutral-neutral cross sections provide a way to extract the interatomic potential over a narrow range in interatomic distances and thus check theoretical models of atom-atom interactions. From the point of view of fusion research, knowledge of atomic cross sections increases our understanding of edge effects, allows improved designs and models of divertors, and refined calculations of neutral density profiles.¹ For these applications the differential cross section at each energy for each process, e.g., elastic, reactive, and ionization, should be known. However, in the energy and density range relevant to magnetic confinement, the elastic scattering cross section is much larger than all the other neutral-neutral processes. The energy range investigated in this experiment is 30–1800 eV. The potentials thus determined are in the repulsive wall region, roughly 0.5 to 2.0 Å depending on the pair. The pairs investigated are: D on He, Ne, Ar, and Kr, and He on He, Ar, and Kr. The technique employed marks the first time a magnetic fusion device has been used to provide basic data of atom-atom collisions.

The cross sections are determined by passing energetic neutral atoms through a gas-filled scattering cell and monitoring the attenuation as a function of pressure in the cell.² The source of the energetic neutrals is the charge exchange efflux from the Princeton large torus (PLT) tokamak.³ The PLT tokamak provides 1 s “shots” of nearly constant 2×10^{15} atoms/cm² s efflux generated by charge exchange of cold gas atoms with hotter plasma ions. These charge-exchange atoms are in the ground state and have an average energy of ~ 250 eV. The great advantage of using the PLT tokamak for studying certain atomic processes is the purity of the efflux and the “brightness” of the emission in the desired energy range as compared with atomic beam techniques.

The detector of the energetic neutrals is the low-energy neutral-atom spectrometer (LENS),^{4,5} a time-of-flight spectrometer with an energy range of 10–2000 eV for deuterium. The minimum detectability threshold for deuterium at 100 eV is 1.0×10^{10} atoms/cm² eV s ster when the time resolution is 1 ms.^{2,6} Since the flux over a wide energy range is

measured virtually simultaneously, and since elastic neutral-neutral collisions dominate at these energies,^{7–10} the dependence of cross section on energy for a particular pair of atoms can be determined during a 1 s discharge, orders of magnitude less time than by other techniques.

Using a pulsed gas valve, a scattering cell between the PLT tokamak and the LENS can be filled within milliseconds with a selected gas. The attainable steady-state pressure range is 1×10^{-4} to 1×10^{-1} Torr as measured by a calibrated Schultz-Phelps gauge. When a scattering gas of density n is present in the cell, some of the neutrals from the tokamak that were directed toward the LENS detector are scattered from the beam. The intensity of neutrals at a given energy $I(E)$, after traversing a length L , in the scattering gas is simply $I(E) = I_0(E) \exp[-nL\sigma(E)]$, where $I_0(E)$ is the initial intensity at energy E , and $\sigma(E)$ is nominally the cross section at that energy. What is actually measured is $\bar{\sigma}_{sc}(E)$, the averaged effective-angle-dependent total scattering cross sec-

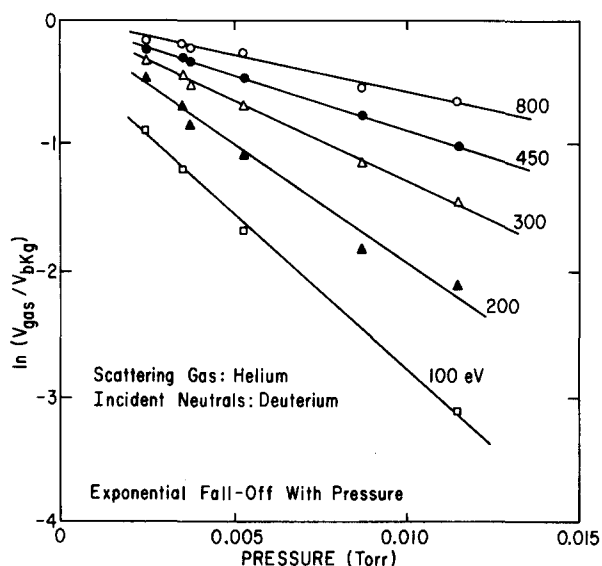


FIG. 1. Comparison of “gas” to “background” charge-exchange efflux ratio vs pressure for five energies of incident deuterium neutrals on six different pressures of helium. The linearity of these curves on the semilog plot indicates that single-event elastic scattering is the dominant attenuation process. The slope of these lines is inversely proportional to $-\bar{\sigma}_{sc}L$.

^{a)} Present address: Nuclear Engineering Department, University of Illinois, Urbana, Illinois 61801.

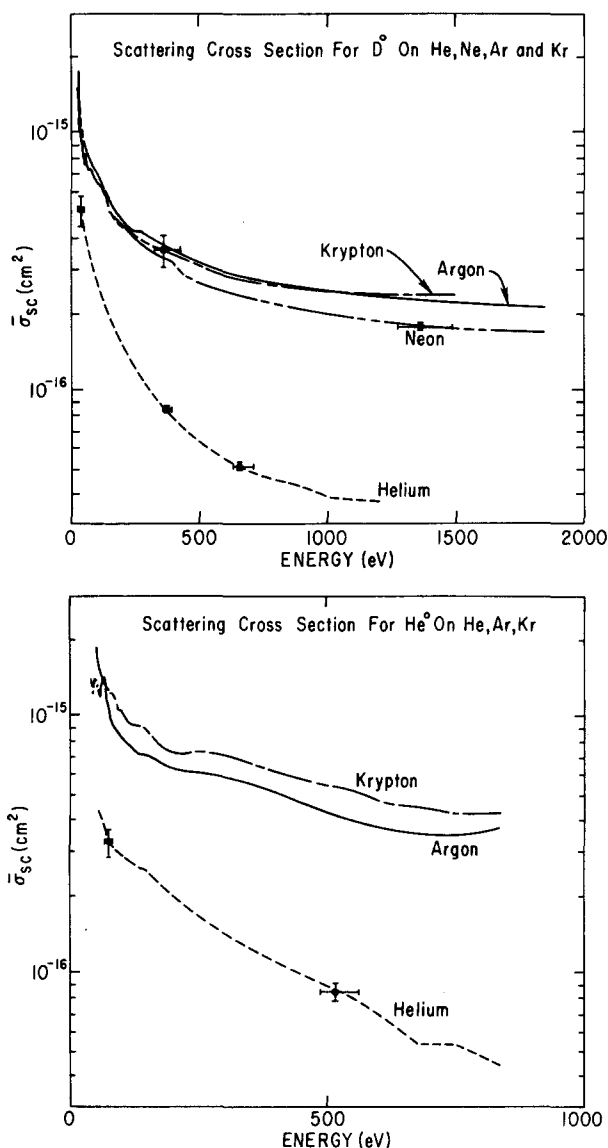


FIG. 2. (a) The error bars for neon and argon at a given energy are the same size as the ones shown for helium at that energy. The krypton error is proportionally larger along the entire curve. (b) The error bars for argon and krypton are the same as the ones shown for helium.

tion. It is an averaged quantity because the scattering cell has finite dimensions; it is effective-angle dependent because deflections smaller than a certain angle are still detected. Further complications arise from scattering events that add particles into the beam.

TABLE I. Effective scattering angles θ_{eff} for the total scattering cross sections presented in Fig. 2, and interatomic potential parameters for the form $V(r) = K r^{-s}$. The potentials are valid between r_{min} and r_{max} . The values of r have about a 10% error.

Incident atom	Target atom	θ_{eff} (mrad)	$s \pm 0.05$	K (max) ($\text{\AA}^s \text{eV}$)	K (min) ($\text{\AA}^s \text{eV}$)	r_{max} (\AA)	r_{min} (\AA)
D	He	19.5	2.60	4.02	0.320	1.29	0.33
D	Ne	22.1	3.45	14.2	1.92	2.33	0.71
D	Ar	23.9	4.45	14.9	2.46	2.19	0.81
D	Kr	24.7	5.20	12.4	2.19	1.31	0.84
He	He	19.5	2.60	5.74	0.457	1.18	0.38
He	Ar	22.6	3.70	28.4	4.14	2.39	1.06
He	Kr	24.1	4.90	47.5	8.28	2.19	1.16

Defining the z axis as the direction along the beam of neutrals, the relationship between the "background" beam intensity observed when no gas is in the scattering cell I_{bkg} and when a gas is present, I_{gas} , is given by an integral over the entire beam path:

$$-\ln \frac{I_{\text{gas}}}{I_{\text{bkg}}} = \int_0^a n(z)\sigma dz + \int_a^{a+b} n(z)\sigma dz + \int_{a+b}^{a+b+c} n(z)\sigma dz, \quad (1)$$

where a is the length of the detector system, b is the length of the scattering cell, and c is the length of the duct to the PLT tokamak.

The density $n(z)$ was calculated at all z for each pressure using the vacuum system transient simulator (VSTS) code.¹¹ The code and pressure gauges show the density in the scattering cell n_{sc} is constant. The scattering cross section that is measured, $\bar{\sigma}_{\text{sc}}$, is not constant along z because $\bar{\sigma}_{\text{sc}}$ is a function of the angular transmission of the apparatus. Letting $d\sigma(\theta, \phi)/d\Omega$ be the differential scattering cross section and θ_{eff} be the effective resolution angle, $\bar{\sigma}_{\text{sc}}$ is defined

$$\bar{\sigma}_{\text{sc}} = \frac{1}{b} \int_a^{a+b} \int_0^{2\pi} \int_{\theta_{\text{eff}}}^{\pi} \frac{d\sigma}{d\Omega}(\theta, \phi) \sin \theta d\theta d\phi dz. \quad (2)$$

Equation (1) can now be written

$$-\ln \frac{I_{\text{gas}}}{I_{\text{bkg}}} = n_{\text{sc}} \sigma_{\text{sc}} L, \quad (3)$$

where $L = b(1 + \alpha)$ and

$$\alpha \equiv \frac{\int_0^a n(z)\sigma dz + \int_{a+b}^{a+b+c} n(z)\sigma dz}{n_{\text{sc}} b \bar{\sigma}_{\text{sc}}}. \quad (4)$$

The correction term α accounts for scattering outside the scattering cell. It was calculated using the VSTS code and following Amdur and Jordan^{2,12} for each pressure and pair of atoms. The value of α was 0.15 ± 0.015 for all combinations except for helium on helium where it was 0.20 ± 0.02 .

The error in the measured quantity $\bar{\sigma}_{\text{sc}}$ is due to uncertainty in effective length, pressure measurement, and counting statistics. Arrival time uncertainty produces an error in energy. At 100 ± 5 eV, e.g., the uncertainty in effective length is 2.0%; the uncertainty in pressure measurement is 5.0%; and the uncertainty due to counting statistics is 7.9%. The counting statistic uncertainty lessens at higher energies, but the uncertainty in energy becomes greater.

When different pressures of the same gas are used in the scattering cell, $\ln(I_{\text{gas}}/I_{\text{bkg}})$ should be directly proportional to the pressure if no multiple scattering or experimental artifact² occurs. Figure 1 shows this linear dependence for deuterium incident on helium. Figures 2(a) and 2(b) show $\bar{\sigma}_{\text{sc}}$ as a function of energy for all the gas pairs measured. For values of $\bar{\sigma}_{\text{sc}}$ to be useful, the effective angle must be known. The calculation is elaborate for a divergent beam.

Two events can change the intensity of a beam of particles when it heads toward a detector through a scattering gas:

(a) Particles that were going to hit the detector are scattered out of the way. Following Jordan,¹³ the cross section for this is called σ_p .

(b) Some particles that were going to miss the detector are scattered into it. This cross section is denoted σ_p^* . When a well-collimated beam is incident on the scatterers, this cross section is ignorably small. Here, where the incident beam is conically shaped with its apex at the end of the scattering cell and its base at the tokamak, σ_p^* can be a major perturbation.

The total cross section determined in this experiment, $\bar{\sigma}_{\text{sc}}$, is

$$\bar{\sigma}_{\text{sc}} = \frac{1}{b} \int_b^{a+b} (\bar{\sigma}_p - \bar{\sigma}_p^*) dz. \quad (5)$$

If the problem is treated classically,¹⁴ an analytic expression for $\bar{\sigma}_{\text{sc}}$ can be found assuming the interaction is governed by a spherical potential $V(r) = Kr^{-s}$.^{2,12,15,16} For the energies and masses of the atomic pairs considered, the analytic expressions for $\bar{\sigma}_p$ and $\bar{\sigma}_p^*$ are

$$\sigma_p = \frac{1}{2} \left[\frac{KF(s)}{E} \right]^{2/s} \int_0^{2\pi} \theta_d^{-2/s} d\phi \quad (6)$$

and

$$\sigma_p^* = \frac{1}{2} \left[\frac{KF(s)}{E} \right]^{2/s} \int_{\phi_{\min}}^{\phi_{\max}} (\theta_{d\min}^{-2/s} - \theta_{d\max}^{-2/s}) d\phi, \quad (7)$$

where ϕ_{\min} , ϕ_{\max} , θ_d , $\theta_{d\min}$, and $\theta_{d\max}$ refer to scattering angles in the gas cell that are generally functions of position, incident and azimuthal scattering angles,² and

$$F(s) = (\pi^{1/2}) \frac{\Gamma(s/2 + 1/2)}{\Gamma(s/2)}. \quad (8)$$

Averaging Eqs. (6) and (7) over the incident angles and area of the cell, and substituting them into Eq. (5) gives the expression for $\bar{\sigma}_{\text{sc}}$:

$$\bar{\sigma}_{\text{sc}} = \pi \left[\frac{KF(s)}{E} \right]^{2/s} \langle \theta^{-2/s} \rangle, \quad (9)$$

where

$$\langle \theta^{-2/s} \rangle \equiv \frac{1}{2\pi b} \times \frac{\int \int_0^{2\pi} \theta_d^{-2/s} d\theta dr - \int \int_{\phi_{\min}}^{\phi_{\max}} (\theta_{d\min}^{-2/s} - \theta_{d\max}^{-2/s}) d\phi dr}{\int dr}. \quad (10)$$

Note that dr has four dimensions: two angles to define the incident beam's direction, and the x and y dimensions of the scattering cell. The effective scattering angle θ_{eff} can now be defined:

$$\theta_{\text{eff}} = \langle \theta^{-2/s} \rangle^{-s/2}. \quad (11)$$

The integral in Eq. (10) requires a quantum correction for very small deflection angles, $\theta_d < \theta_c$. These critical angles typically have values of 1 to 5 mrad, though classical results may still mimic the quantum results for even smaller angles.¹⁷ A semiclassical cutoff angle,^{18,19} θ_{co} , somewhat below θ_c was used in the calculation of θ_{eff} . The results are insensitive to θ_{co} because $\theta_{\text{eff}} \gg \theta_{\text{co}}$.

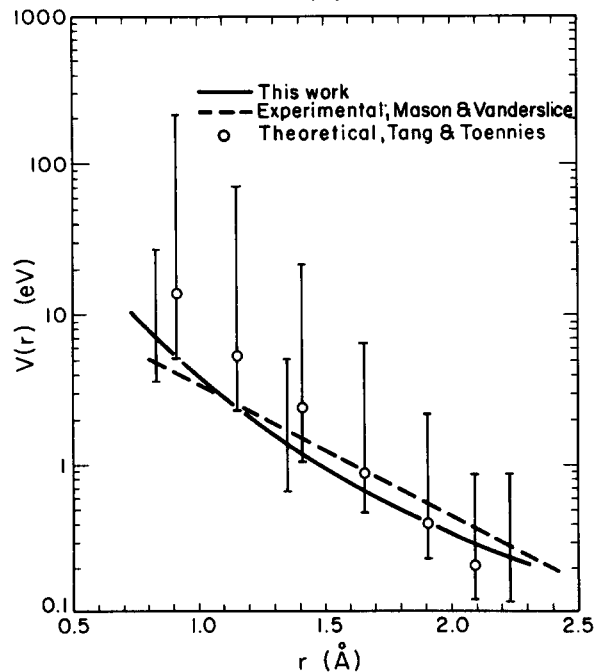
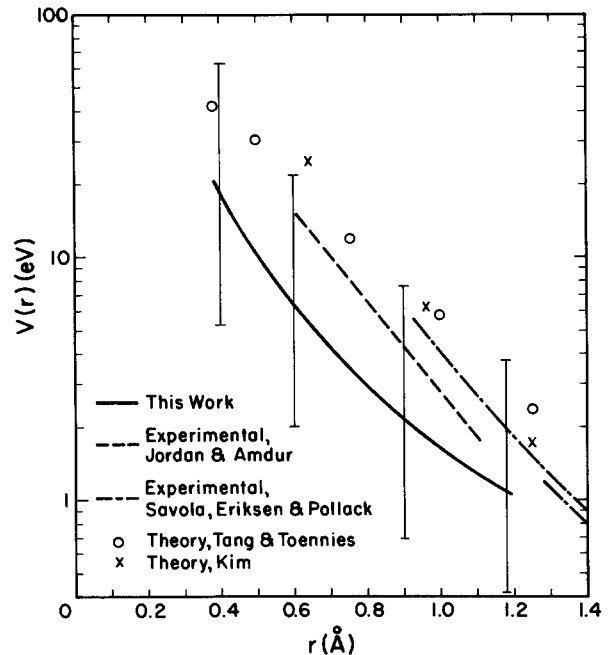


FIG. 3. (a) Interatomic potential for He on He. Jordan and Amdur (Ref. 13) and Savola, Eriksen, and Pollack (Ref. 24) used total scattering cross section measurements. Tang and Toennies (Ref. 22) used self-consistent field theory. Kim (Ref. 23) used the variational principle. (b) This work: interatomic potential for D on Ne. Others: interatomic potential for H on Ne. Mason and Vanderslice (Ref. 25) deduced the potential from total scattering cross-section measurements of other pairs. Tang and Toennies (Ref. 22) used self-consistent-field theory.

For very simple geometries, Eq. (10) can be solved analytically.²⁰ But for the geometry used in this experiment the integral was broken into 81 regions and evaluated² with the aid of the national magnetic fusion energy computer center Cray I computer.

To find s from the data, Eq. (9) can be put into linear form and solved graphically. In principle, K can also be found, but the error associated with it is quite large. The validity limits for the interatomic potential's range come from the minimum and maximum scattering cross section observed.¹⁴ The effective angles and the potential parameters for all the pairs of atoms studied are listed in Table I. The results do overlap *ab initio* theoretical calculations.^{21,22} Figure 3(a) shows the experimentally determined interatomic potential for He on He; Fig. 3(b) shows it for D on Ne. Graphical comparisons for the other atomic pairs can be found in Ref. 2. The error bars shown for this work represent the maximum and minimum K values consistent with the data. Some theoretical potential calculations^{22,23} and other experimentally determined He-He potentials,^{13,24} and H-Ne potentials²⁵ are shown for comparison.

In summary, total scattering cross sections for neutral D on He, Ne, Ar, and Kr, and for neutral He on He, Ar, and Kr, have been determined in the energy range of 30–1800 eV for an effective angle of approximately 20 mrad. The experiment shows the utility of the tokamak for studying atomic scattering processes at low energies.

ACKNOWLEDGMENTS

We wish to thank Dr. J. Hosea for his encouragement and the PLT staff and crew for their technical support. This

work was supported by the Fannie and John Hertz Foundation and US DOE Contract No. DE-AC02-76-CHO-3073.

- ¹D. Post, in *Physics of Ion-Ion and Electron-Ion Collisions*, edited by F. Brouillard and J. W. McGowan (Plenum, New York, 1983).
- ²D. N. Ruzic, Ph. D. thesis, Princeton University, 1984.
- ³D. Grove *et al.*, Proc. 6th Inter. Conf. on Physics and Controlled Thermonuclear Fusion Research, Berchtesgaden, West Germany, 1976, p. 21.
- ⁴D. E. Voss, Ph. D. thesis, Princeton University, 1980.
- ⁵D. E. Voss and S. A. Cohen, Rev. Sci. Instrum. **53**, 1969 (1982).
- ⁶D. Ruzic, T. K. Chu, S. Cohen, D. Heifetz, and J. Stevens, Bull. Am. Phys. Soc. **27**, 1070 (1982).
- ⁷R. Morgenstern, M. Barat, and D. C. Lorents, J. Phys. B **6**, L330 (1973).
- ⁸C. Benoit and J. P. Gauyacq, J. Phys. B **6**, L391 (1976).
- ⁹N. Noda, J. Phys. Soc. Jpn. **41**, 625 (1976).
- ¹⁰B. Van Zyl, T. Q. Le, H. Neumann, and R. C. Amme, Phys. Rev. A **15**, 1871 (1977).
- ¹¹J. Sredniawski, S. S. Medley, and H. Fishman, Princeton Plasma Physics Laboratory Report PPPL-TM-326 (1979).
- ¹²I. Amdur and J. E. Jordan, Adv. Chem. Phys. **10**, 29 (1967).
- ¹³J. E. Jordan and I. Amdur, J. Chem. Phys. **46**, 165 (1967).
- ¹⁴E. A. Mason and J. T. Vanderslice, *Atomic and Molecular Processes*, edited by D. R. Bates (Academic, New York, 1962), Chap. 17.
- ¹⁵I. Amdur and H. Pearlman, J. Chem. Phys. **9**, 503 (1941).
- ¹⁶B. H. Bransden and C. J. Joachain, *Physics of Atoms and Molecules* (Longman, London, 1983), Chap. 13.
- ¹⁷E. A. Mason, J. T. Vanderslice, and C. J. G. Raw, J. Chem. Phys. **40**, 2153 (1964).
- ¹⁸K. W. Ford and J. A. Wheeler, Ann. Phys. **7**, 259 (1959).
- ¹⁹R. B. Bernstein, Adv. Chem. Phys. **53**, 50 (1970).
- ²⁰I. Amdur, J. E. Jordan, and S. O. Colgate, J. Chem. Phys. **34**, 1525 (1961).
- ²¹W. D. Wilson and C. L. Bisson, Sandia Laboratories Report SCL-DC-70-45, 1970.
- ²²K. T. Tang and J. P. Toennies, J. Chem. Phys. **66**, 1469 (1977).
- ²³D. Y. Kim, Z. Phys. **166**, 359 (1962).
- ²⁴W. J. Savola, Jr., F. J. Eriksen, and E. Pollack, Phys. Rev. A **7**, 932 (1973).
- ²⁵E. A. Mason and J. T. Vanderslice, J. Chem. Phys. **22**, 1070 (1958).